

## Casson Hybrid Nanofluid Natural Convection in Trapezoidal Cavity containing a Partially Heated Wall

Norihan Md Arifin<sup>1,2,\*</sup>, Habibis Saleh<sup>3</sup>, Ishak Hashim<sup>4</sup>, Fatin Munirah Azizul<sup>4</sup>

<sup>1</sup> Department of Mathematics and Statistics, Faculty of Science, Universiti Putra Malaysia, Serdang, Selangor 43400 UPM, Malaysia

<sup>2</sup> Institute for Mathematical Research, Universiti Putra Malaysia, Serdang Selangor 43400 UPM, Malaysia

<sup>3</sup> Mathematics Education Department, Universitas Islam Negeri Sultan Syarif Kasim, 28293, Pekanbaru, Indonesia

<sup>4</sup> Department of Mathematical Sciences, Faculty of Science and Technology, Universiti Kebangsaan Malaysia, 43600 UKM Bangi, Malaysia

### ARTICLE INFO

#### Article history:

Received 15 April 2022

Received in revised form 18 September 2022

Accepted 27 September 2022

Available online 20 October 2022

#### Keywords:

Natural convection flow; Casson hybrid nanofluid; trapezoidal cavity; finite element method

### ABSTRACT

A computational analysis has been performed for Casson hybrid nanofluid natural convection heat transfer in trapezoidal cavity containing a partially heated at bottom wall, and the incline walls are set to be at the cold temperature while the top wall is supposed to be adiabatic. The hybrid nanoparticles, alumina and copper are dispersed in ethylene glycol and water mixture has been used as a working fluid. The finite element method is used to solve the nondimensional governing partial differentials equations. The numerical results are carried out for different governing parameters such as Casson parameter ( $\gamma = 0.1 - 1$ ) Rayleigh number ( $Ra = 10^4 - 10^6$ ) and hybrid nanoparticles volume fraction ( $\varphi = 0.01 - 0.05$ ) and heated zone length. The influence of these parameters on streamlines, isotherms, velocities and average Nusselt number will be the focus in this study.

## 1. Introduction

The study on the heat and mass transfer characteristics about the convection of non-Newtonian fluids is of much importance because of the practical and industrial applications, and such fluids involve honey, blood, greases and oils. The convective heat transfer mechanisms of the non-Newtonian of Casson fluid are the subject of considerable works and are well understood today since of wide applications in food processing, energy production, drilling operation, metallurgy and bio-engineering operations. Many researchers defined the non-Newtonian of Casson fluid model as a shear thinning liquid which is assumed to have an infinite viscosity at zero rate of shear. There are also several numerical studies to better understand the mechanism of heat transfer enhancement for Casson fluid flow with various surfaces and geometries was discussed in the literature [1-12].

Cavities and enclosures are becoming of the most interesting subject among different industries. A detail review on the buoyancy induced flows in trapezoidal enclosures is reported by Mahat *et al.*, [13], Sheremet *et al.*, [14], and Alsabery *et al.*, [15]. Natural-convective flow containing non-

\* Corresponding author.

E-mail address: [norihana@upm.edu.my](mailto:norihana@upm.edu.my)

<https://doi.org/10.37934/arfmts.100.2.7895>

Newtonian nanofluid inside trapezoidal enclosure with sinusoidal walls temperature was studied numerically by Alsabery *et al.*, [16]. Pop and Sheremet [17] obtained numerical results for free-convective Casson fluid in a differentially heated square cavity. Casson fluid natural convective flow inside trapezoidal cavity with partially heated bottom surface was analyzed by Hamid *et al.*, [18]. Later, Aneja *et al.*, [19] have presented the natural convective Casson fluid model in a partially heated square porous cavity. Their results demonstrated that the flow circulation and heat transfer increases with an increment values of Darcy number and Casson fluid parameter.

Recent developments in nanotechnology offers innovative way to enhance heat transfer rate. The addition of higher-thermal-conductivity hybrid nanoparticles such as  $\text{Al}_2\text{O}_3$ , Cu, Ag and  $\text{TiO}_2$  to the convectonal fluid like water, ethylene glycol and oil is a promising technique for enhancing heat transfer. Heat transfer enhancement in fluids containing nanoparticles was first determined by Choi and Eastman [20]. They observed that the thermal conductivity performances of conventional fluids improved when solid nanoparticles are added. After their work, massive research has been theoretically and experimentally conducted to improve the heat transfer properties of the fluids. Thermal conductivity of alumina and copper oxide nanofluids was measured by Mintsa *et al.*, [21] and they revealed that the effective thermal conductivity increases with a rise in particle addition. Saleh *et al.*, [22] investigated the problem of natural-convective flow inside trapezoidal enclosure containing water–copper and water–alumina nanofluids. Later, Nasrin and Parvin [23] obtained numerical results for natural-convective flow inside trapezoidal enclosure containing water–copper nanofluids and the effects of Prandtl number and aspect ratio on the fluid flow were performed. On the other hand, Buongiorno approach nanofluid model has been used by Sheremet *et al.*, [14] for natural-convective fluids flow in a porous right-angle trapezoidal cavity. Miroshnichenko *et al.*, [24] analyzed MHD natural-convective flow of water based copper oxide nanofluid in trapezoidal cavity where the inclined wall is heated and they found that the reduction of heat transfer with the increasing Hartmann number, while by adding nanoparticles to the base fluid led to significant enhancement of heat transfer. The results show that the heat transfer rate inside the cavity increase due to increase in the volume fraction of nanoparticles.

Hybrid nanofluid is developed to boost the thermal performance of convectonal fluids and nanofluids. In hybrid nanofluid, the combination two or more hybrid nanoparticles in the base fluid to provide higher effective thermal conductivity. The concept of using hybrid nanofluids have gained more research attention in recent year. Hybrid nanofluids correlations for thermal conductivity was discussed in detail by Takabi and Salehi [25], Tayebi and Chamka [26] and Ghalambaz *et al.*, [27]. Alshuraiaan and Pop [28] investigated the enhancement of mixed convection heat transfer in a trapezoidal cavity containing flexible bottom wall filled with alumina-copper-copper/water hybrid nanofluid. Recently, Sedeghi *et al.*, [29] reviewed and summarized the findings of the published literature on enhancement of natural convection in various enclosures filled using nanofluid.

Motivated by the work cited earlier, the problems of natural-convective flow inside trapezoidal cavity filled with Casson hybrid nanofluid have not been studied yet. Therefore, in the present study, a numerical analysis of natural-convective fluid flow and heat transfer in a partially heated trapezoidal cavity filled with hybrid Casson nanofluid is reported. The hybrid nanofluid model consists of alumina and copper in mixture of ethylene glycol and water as a base Casson fluid. Roles of Rayleigh number ( $Ra$ ), hybrid nanoparticles volume fraction ( $\varphi$ ), Casson parameter ( $\gamma$ ) and heated surface length ( $a$ ) are demonstrated.

## 2. Problem Formulation

The schematic diagram of the trapezoidal enclosure with Casson hybrid nanofluid fluid containing alumina ( $\text{Al}_2\text{O}_3$ ) and copper (Cu) hybrid nanoparticles in ethylene glycol (EG) and water (W) mixture as a base fluid is shown in Figure 1.

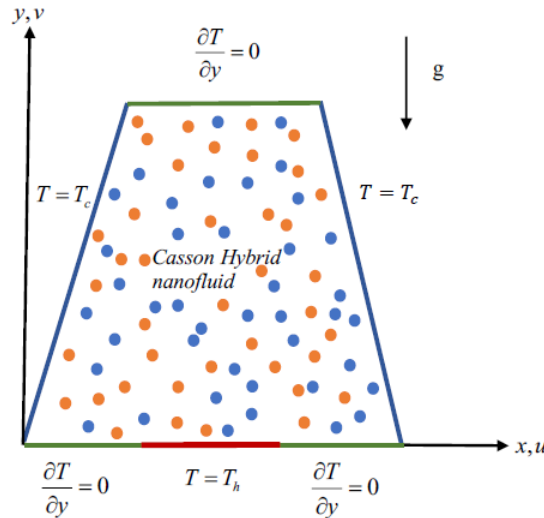


Fig. 1. Sketch of the physical model problem

The higher temperature  $T_h$  is imposed partially on the center of the bottom wall and the cold temperature are imposed to the incline walls. Meanwhile, the top wall and the portion of the bottom wall are supposed to be adiabatic. The influence of hot area on fluid flow and heat transfer characteristics are observed for various length of heated area at the bottom surface. The buoyancy forces owed to the variance heating are performing on the fluid. We consider the variation of density with the help of Boussinesq's approximation. The following dimensional system of equations for Casson hybrid nanofluid [18]

$$\frac{\partial u}{\partial x} + \frac{\partial v}{\partial y} = 0, \quad (1)$$

$$u \frac{\partial u}{\partial x} + v \frac{\partial u}{\partial y} = \frac{1}{\rho_{hnf}} \frac{\partial p}{\partial x} + \frac{\mu_{hnf}}{\rho_{hnf}} \left( 1 + \frac{1}{\gamma} \right) \left( \frac{\partial^2 u}{\partial x^2} + v \frac{\partial^2 u}{\partial y^2} \right), \quad (2)$$

$$u \frac{\partial v}{\partial x} + v \frac{\partial v}{\partial y} = \frac{1}{\rho_{hnf}} \frac{\partial p}{\partial x} + \frac{\mu_{hnf}}{\rho_{hnf}} \left( 1 + \frac{1}{\gamma} \right) \left( \frac{\partial^2 v}{\partial x^2} + v \frac{\partial^2 v}{\partial y^2} \right) + \frac{(\rho\beta)_{hnf}}{\rho_{hnf}} g(T - T_c), \quad (3)$$

$$u \frac{\partial T}{\partial x} + v \frac{\partial T}{\partial y} = \alpha_{hnf} \left( \frac{\partial^2 T}{\partial x^2} + v \frac{\partial^2 T}{\partial y^2} \right) \quad (4)$$

The boundary conditions

$$\text{On top wall: } u = v = 0, \frac{\partial T}{\partial y} = 0, y = 1. \quad (5)$$

On bottom wall:  $u = v = 0$ ,

$$\begin{cases} \frac{\partial T}{\partial y} = 0, & 0 < x < \frac{(1-a)L}{2}, y = 0, \\ T = T_h, & \frac{1-a}{2} < x < \frac{(1+a)L}{2}, y = 0, \\ \frac{\partial T}{\partial y} = 0, & \frac{(1+a)L}{2} < x < 1, y = 0. \end{cases} \quad (6)$$

On right and left inclined wall,  $u = v = 0, T = T_c$ . (7)

The thermal properties of base fluid and empirical correlation for hybrid nanofluid is given in Table 1 [25-27].

**Table 1**  
 Thermophysical properties correlations

Properties	Hybrid Nanofluid correlations
Density	$\rho_{hnf} = \varphi_{Al_2O_3}\rho_{Al_2O_3} + \varphi_{Cu}\rho_{Cu} + (1 - \varphi)\rho_f$ , where $\varphi = \varphi_{Al_2O_3} + \varphi_{Cu}$
Heat Capacity	$(\rho C_p)_{hnf} = \varphi_{Al_2O_3}(\rho C_p)_{Al_2O_3} + \varphi_{Cu}(\rho C_p)_{Cu} + (1 - \varphi)(\rho C_p)_f$
Dynamic Viscosity	$\mu_{hnf} = \mu_f(1 - \varphi_{Al_2O_3} - \varphi_{Cu})^{-2}$
Thermal diffusivity	$\alpha_{hnf} = \frac{k_{hnf}}{(\rho C_p)_{hnf}}$
Thermal Conductivity	$\frac{k_{hnf}}{k_f} = \frac{\left[\left(\frac{\varphi_{Al_2O_3}k_{Al_2O_3} + \varphi_{Cu}k_{Cu}}{\varphi}\right) + 2k_f + 2(\varphi_{Al_2O_3}k_{Al_2O_3} + \varphi_{Cu}k_{Cu}) - 2\varphi k_f\right]}{\left[\left(\frac{\varphi_{Al_2O_3}k_{Al_2O_3} + \varphi_{Cu}k_{Cu}}{\varphi}\right) + 2k_f - (\varphi_{Al_2O_3}k_{Al_2O_3} + \varphi_{Cu}k_{Cu}) + \varphi k_f\right]}$
Electrical Conductivity	$\frac{\sigma_{hnf}}{\sigma_f} = \frac{\left[\left(\frac{\varphi_{Al_2O_3}\sigma_{Al_2O_3} + \varphi_{Cu}\sigma_{Cu}}{\varphi}\right) + 2\sigma_f + 2(\varphi_{Al_2O_3}\sigma_{Al_2O_3} + \varphi_{Cu}\sigma_{Cu}) - 2\varphi\sigma_f\right]}{\left[\left(\frac{\varphi_{Al_2O_3}\sigma_{Al_2O_3} + \varphi_{Cu}\sigma_{Cu}}{\varphi}\right) + 2\sigma_f - (\varphi_{Al_2O_3}\sigma_{Al_2O_3} + \varphi_{Cu}\sigma_{Cu}) + \varphi\sigma_f\right]}$

The thermophysical properties of ethylene glycol/water (EGW) and solid hybrid nanoparticles Alumina ( $Al_2O_3$ ) and Copper (Cu) are stated in Table 2.

**Table 2**  
 Thermophysical properties

Properties	Ethylene Glycol/Water	Alumina	Copper
$\rho$ (kg/m <sup>3</sup> )	1018	3970	8933
$C_p$ (J/kgK)	4004	752	383
$k$ (W/mK)	0.53	36.6	401.7
$\sigma$ (S/m)	$5.5 \times 10^{-6}$	$35 \times 10^6$	$59.6 \times 10^6$
$\beta$ (1/K)	$21 \times 10^{-5}$	$0.85 \times 10^{-5}$	$1.67 \times 10^{-5}$

Considering the following parameters

$$(X, Y) = \frac{(x, y)}{L}, (U, V) = \frac{(uL, vL)}{\alpha_{hnf}}, P = \frac{\nu L^2}{\rho_f \alpha_{hnf}^2}, (T - T_c) = (T_h - T_c)\theta. \quad (8)$$

The governing Eq. (1) to Eq. (3) are reduced to the following set of dimensionless equation

$$U \frac{\partial U}{\partial X} + V \frac{\partial U}{\partial Y} = -\frac{\partial P}{\partial X} + Pr \frac{\nu_{hnf}}{\nu_f} \left(1 + \frac{1}{\gamma}\right) \left(\frac{\partial^2 U}{\partial X^2} + \frac{\partial^2 U}{\partial Y^2}\right), \quad (9)$$

$$U \frac{\partial V}{\partial X} + V \frac{\partial V}{\partial Y} = -\frac{\partial P}{\partial X} + \text{Pr} \frac{\nu_{hnf}}{\nu_f} \left(1 + \frac{1}{\gamma}\right) \left(\frac{\partial^2 V}{\partial X^2} + \frac{\partial^2 V}{\partial Y^2}\right) + \frac{(\rho\beta)_{hnf}}{\rho_{hnf}\beta_f} \text{PrRa}\theta, \quad (10)$$

$$U \frac{\partial \theta}{\partial X} + V \frac{\partial \theta}{\partial Y} = \frac{\alpha_{hnf}}{\alpha_f} \left(\frac{\partial^2 \theta}{\partial X^2} + \frac{\partial^2 \theta}{\partial Y^2}\right), \quad (11)$$

where  $\text{Pr} = \mu_f(\rho C_p)_f / \rho_f k_f$  is the Prandtl number and  $\text{Ra} = g(\rho\beta)_f(T_h - T_c)(\rho C_p)_f L^3 / \mu_f k_f$  is the Rayleigh number. The corresponding non-dimensional boundary conditions are

On top wall:  $U = V = 0, \frac{\partial \theta}{\partial Y} = 0, Y = 1$ .

On bottom wall:  $U = V = 0,$

$$\begin{cases} \frac{\partial \theta}{\partial Y} = 0, & 0 < X < \frac{(1-a)L}{2}, Y = 0, \\ \theta = 1, & \frac{1-a}{2} < X < \frac{(1+a)L}{2}, Y = 0, \\ \frac{\partial \theta}{\partial Y} = 0, & \frac{(1+a)L}{2} < X < 1, Y = 0. \end{cases} \quad (12)$$

On right and left inclined wall,  $U = V = 0, \theta = 0. U = V = 0, \theta = 0$ .

The local Nusselt number,  $Nu_x$  can be expressed in nondimensional form by using Eq. (4) as

$$Nu_x = \frac{k_{hnf}}{k_f} \frac{\partial \theta}{\partial Y} \Big|_{Y=0},$$

and the average Nusselt number  $Nu_{avg}$  over the heated bottom wall is described as

$$Nu_{avg} = \frac{1}{S} \int_S Nu_x.$$

### 3. Computational Procedure

The governing Eq. (8) to Eq. (10) along with the associated boundary conditions (11) is solved using the Galerkin weighted residual along with finite element methods. This technique is a well-accepted approach and verified comprehensively by Alsabery *et al.*, [15]. The finite element mesh of the present problem is display in Figure 2. Five different finite element meshes have been considered and the value of average Nusselt number are carried out and presented in Table 3. Therefore, all the simulations have been carried out at mesh size extra fine with 13856 elements grid system. To show the validity of the present model, the comparison numerical works with Hamid *et al.*, [18] as demonstrated in Figure 3 and Figure 4 for the natural-convective Casson fluids in trapezoidal cavity containing a partially heated at bottom wall. The iteration is reported until the normalized residual of the governing equations less than  $10^{-6}$ .

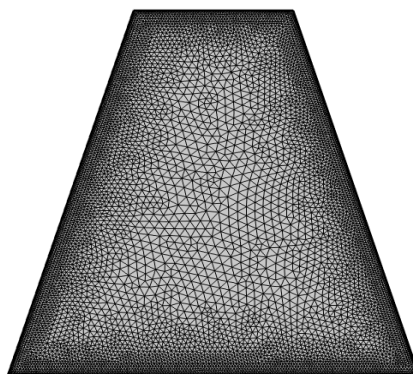


**Fig. 2.** Example of Mesh generation

**Table 3**

Comparison of  $Nu_{avg}$  for different grid resolution at  $Ra = 10^5$ ,  $\gamma = 0.1$ ,  $\phi = 0.05$  and  $Pr = 6.2$

Predefined mesh size	Domain elements	Boundary elements	$Nu_{avg}$	CPU time (s)
Normal	1171	101	3.5767	10
Fine	1855	127	3.6269	10
Finer	5239	269	3.7943	12
Extra fine	13856	520	3.9049	20
Extremely fine	19644	520	3.9047	25

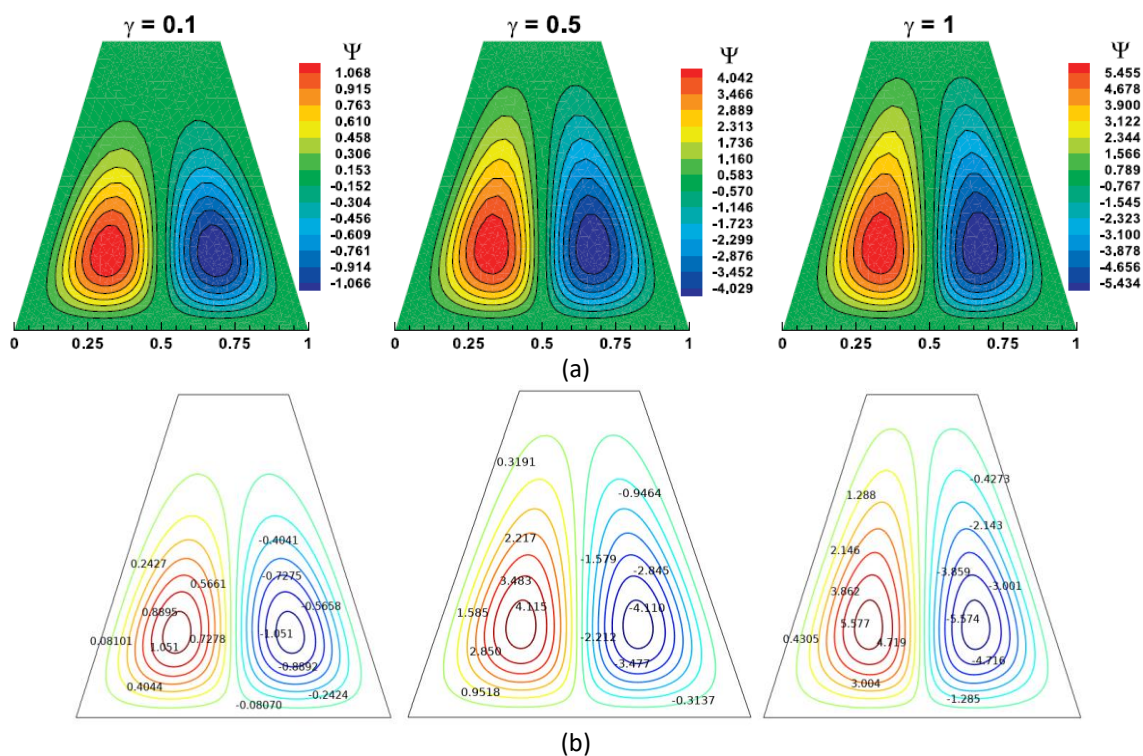


**Fig. 3.** Comparison of streamlines reported by Hamid *et al.*, [18] (a) and present study (b) for partially heated ( $\alpha = 0.4$ ) with  $Ra = 10^5$  and  $Pr = 20$

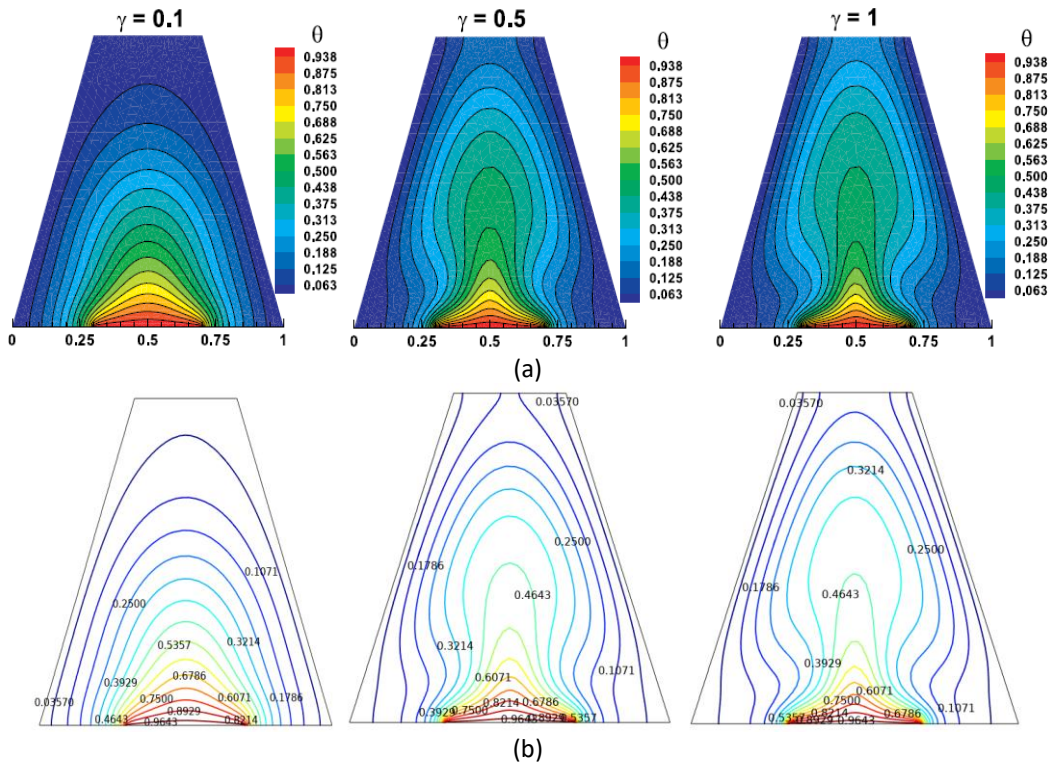


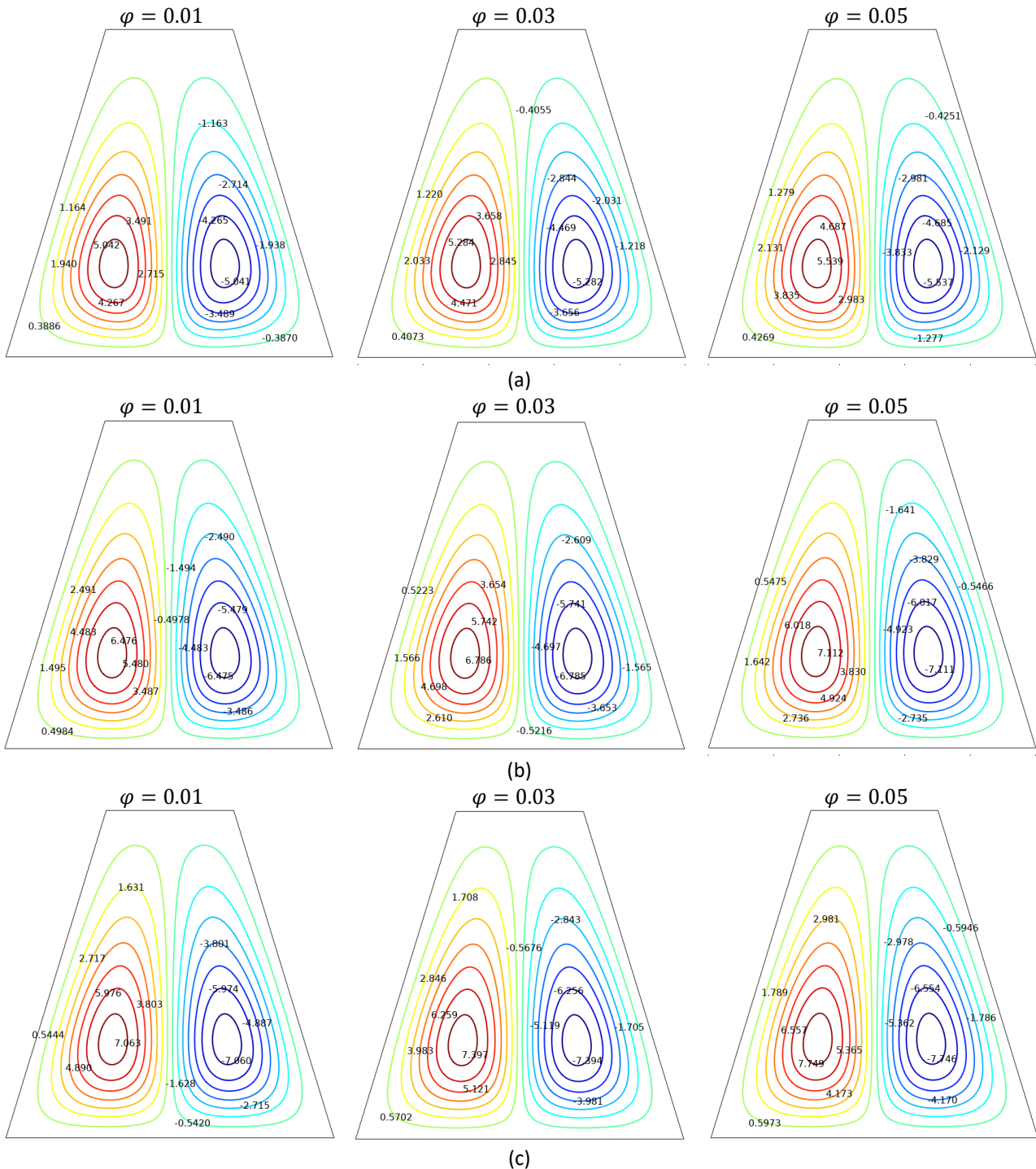
**Fig. 4.** Comparison of isotherms reported by Hamid *et al.*, [18] (a) and present study (b) for partially heated ( $a = 0.4$ ) with  $Ra = 10^5$  and  $Pr = 20$

#### 4. Results and Discussion

This section performs numerical outcome of the fluid flow and temperature distribution within the trapezoidal cavity via streamlines, isotherms and average Nusselt number. The trapezoidal cavity was filled with Casson hybrid nanofluid ( $Al_2O_3 - Cu/EGW$ ). The hybrid nanofluid model in this study consists of alumina and copper in ethylene glycol and water mixture as a base Casson fluid, where alumina ( $\varphi_{Al_2O_3} = 0.01$ ) is the first nanoparticle dispersed into the ethylene glycol and water mixture and then continued by the dispersion of copper ( $0.01 \leq \varphi_{Cu} \leq 0.04$ ). So, in this study, alumina volume fraction is set to be fixed and copper volume fraction is set to be varied accordingly. The analysis is carried out for the variation of Casson parameter ( $\gamma = 0.1 - 1$ ), Rayleigh number ( $Ra = 10^4 - 10^6$ ) and heated surface length ( $a = 0.2, 0.4, 0.6$ ) at fixed Prandtl number ( $Pr = 6.2$ ).

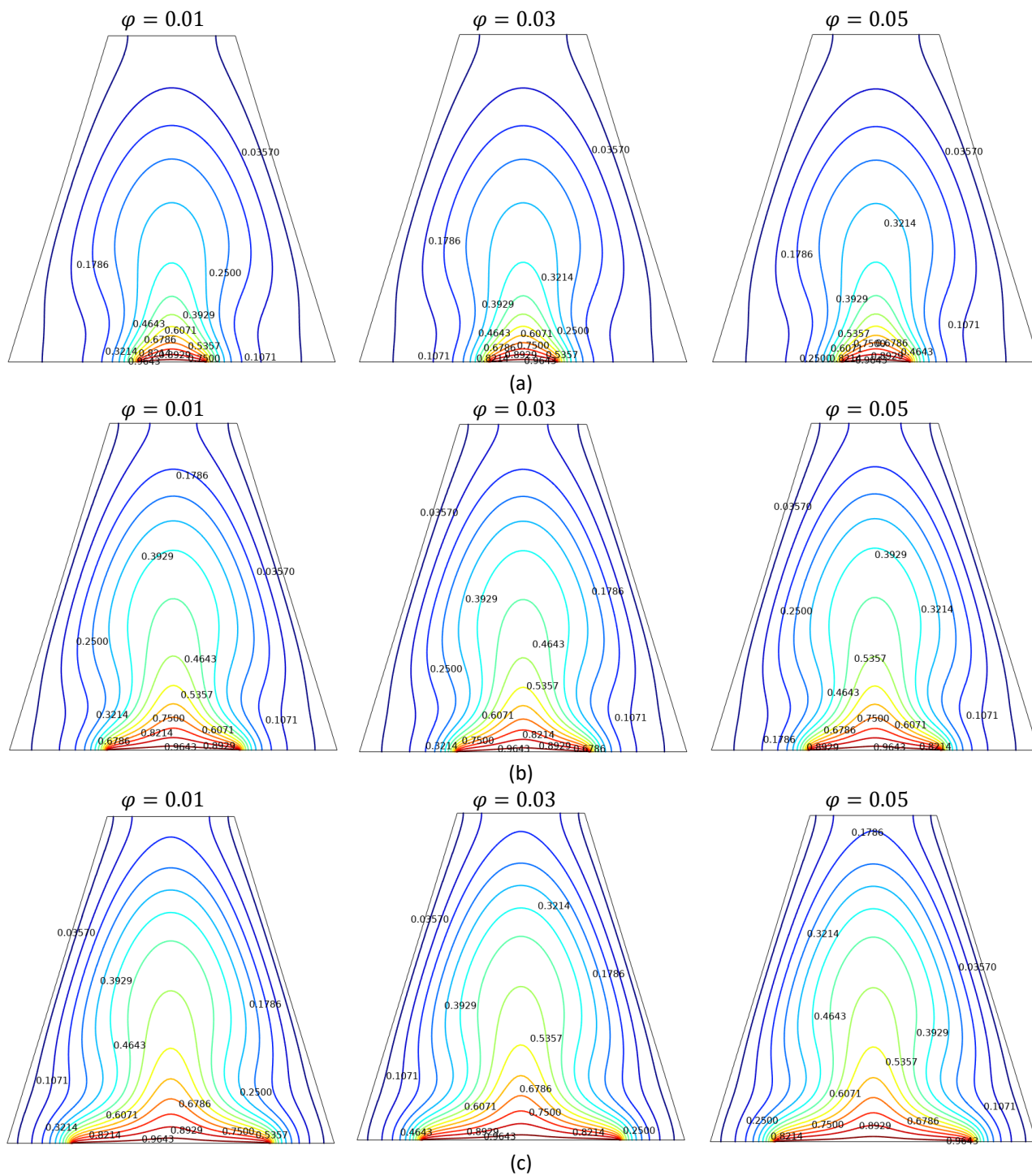
The streamline and isotherm contours in Figure 5 to Figure 11 show the effects of hybrid nanoparticles volume fraction, Rayleigh number, heated surface length and Casson parameter on the flow structure, thermal fields and velocities. It is observing that the presence of circular streamlines has two large vortices with different orientation, where one of them flows clockwise (negative sign) fluid circulation and the other flows anti-clockwise fluid circulation. Figure 5 and Figure 6 demonstrates the streamlines and isotherms contours for  $Ra = 10^5$ ,  $\gamma = 0.5$  and different length of heated zone and hybrid nanoparticles volume fraction. As seen, changing the heated zone length has no impact on the streamline since the flow pattern show the symmetrical distribution. It can be noted that the distribution of streamlines contour maps almost similar for different values of particles volumes fraction. The hybrid nanoparticles added in the base fluid alters the heat transfer properties of the hybrid nanofluid and it is reflecting the strength of flow circulation. Meaning that, increasing  $\varphi$ , raised the convective heat transfer due to increasing flow circulation. Furthermore, Figure 6 shows the influence of the heated zone length on the temperature contours. It can be seen the isotherms pattern is more concentrated near the heated surface and the maximum isotherms amount is at the

heated bottom cavity. The isotherm amount is change based on the heated surface length and the isotherm are occupying the entire cavity with increasing the heated zone length. Figure 7 and Figure 8 demonstrates the effect of applying various values of particles volume fraction and heated zone on the behavior of the velocities  $U$  and  $V$ . For the velocities, the strength of the circulation increases with the increase of the hybrid particles volume fraction.

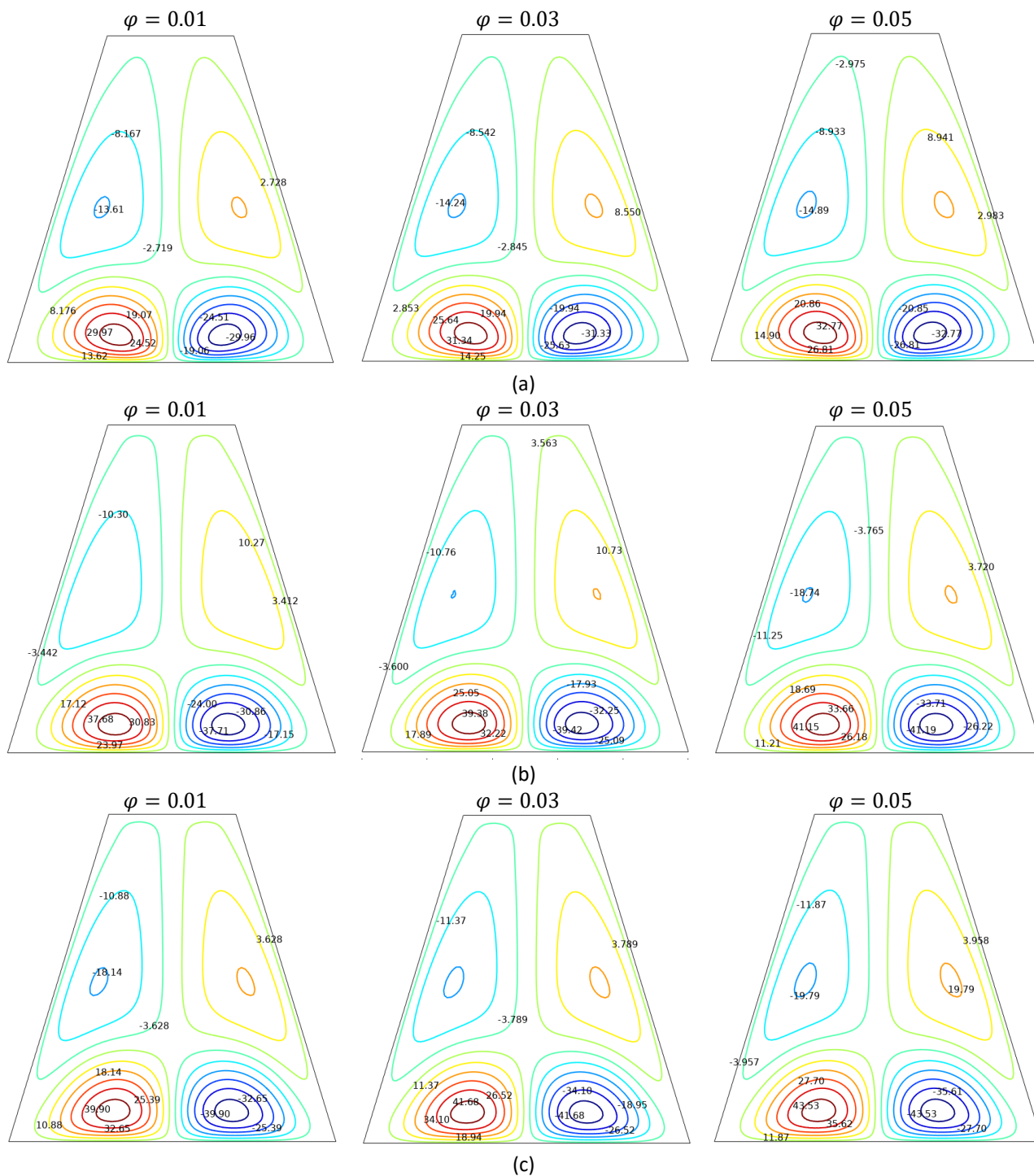


**Fig. 5.** Streamlines contours for different  $\alpha$  and  $\phi$  at  $Ra = 10^5$  and  $\gamma = 1$ ; (a)  $\alpha = 0.2$ , (b)  $\alpha = 0.4$ , (c)  $\alpha = 0.6$

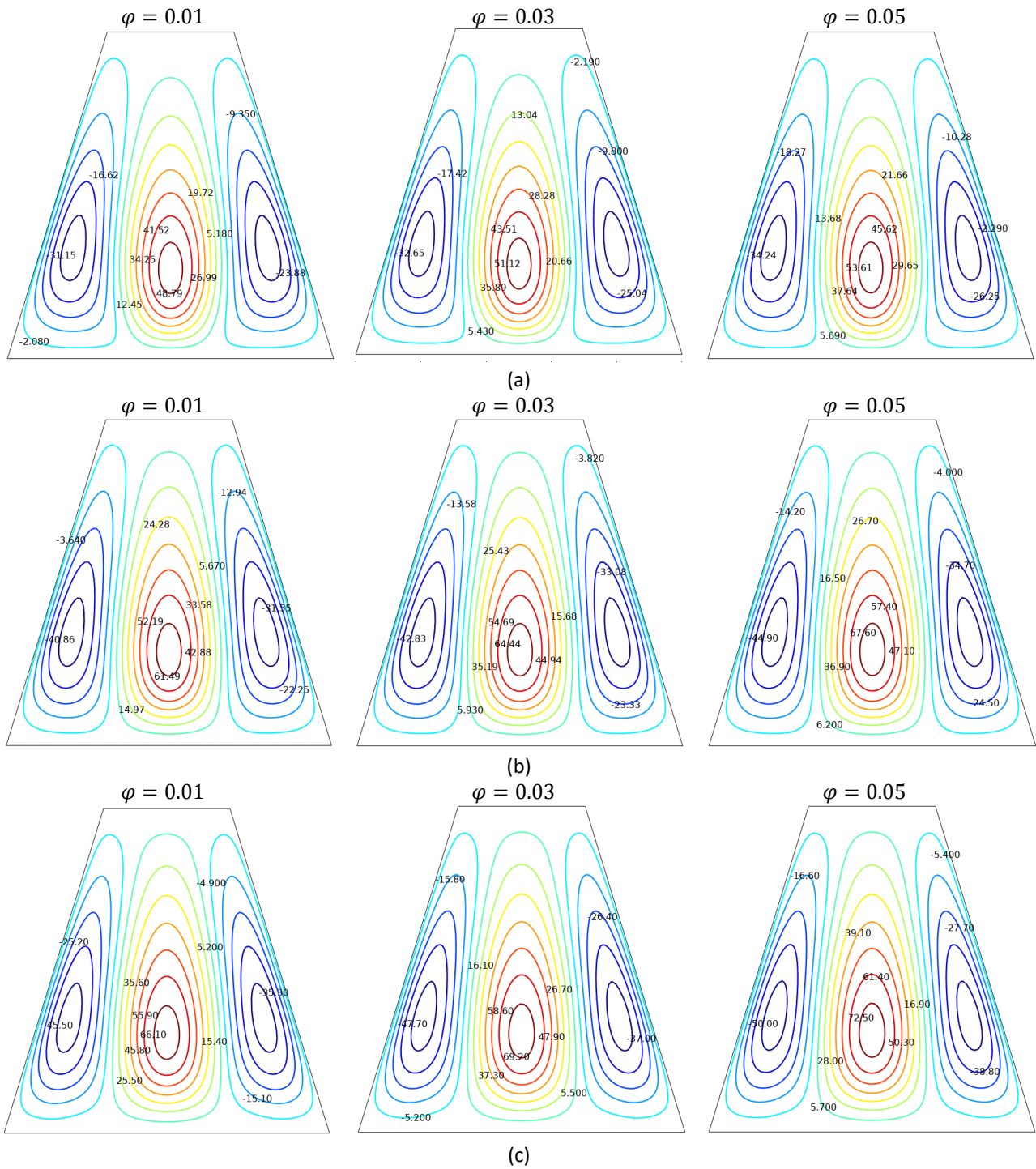




**Fig. 6.** Isotherms contours for different  $a$  and  $\varphi$  at  $Ra = 10^5$  and  $\gamma = 1$ ; (a)  $a = 0.2$ , (b)  $a = 0.4$ , (c)  $a = 0.6$



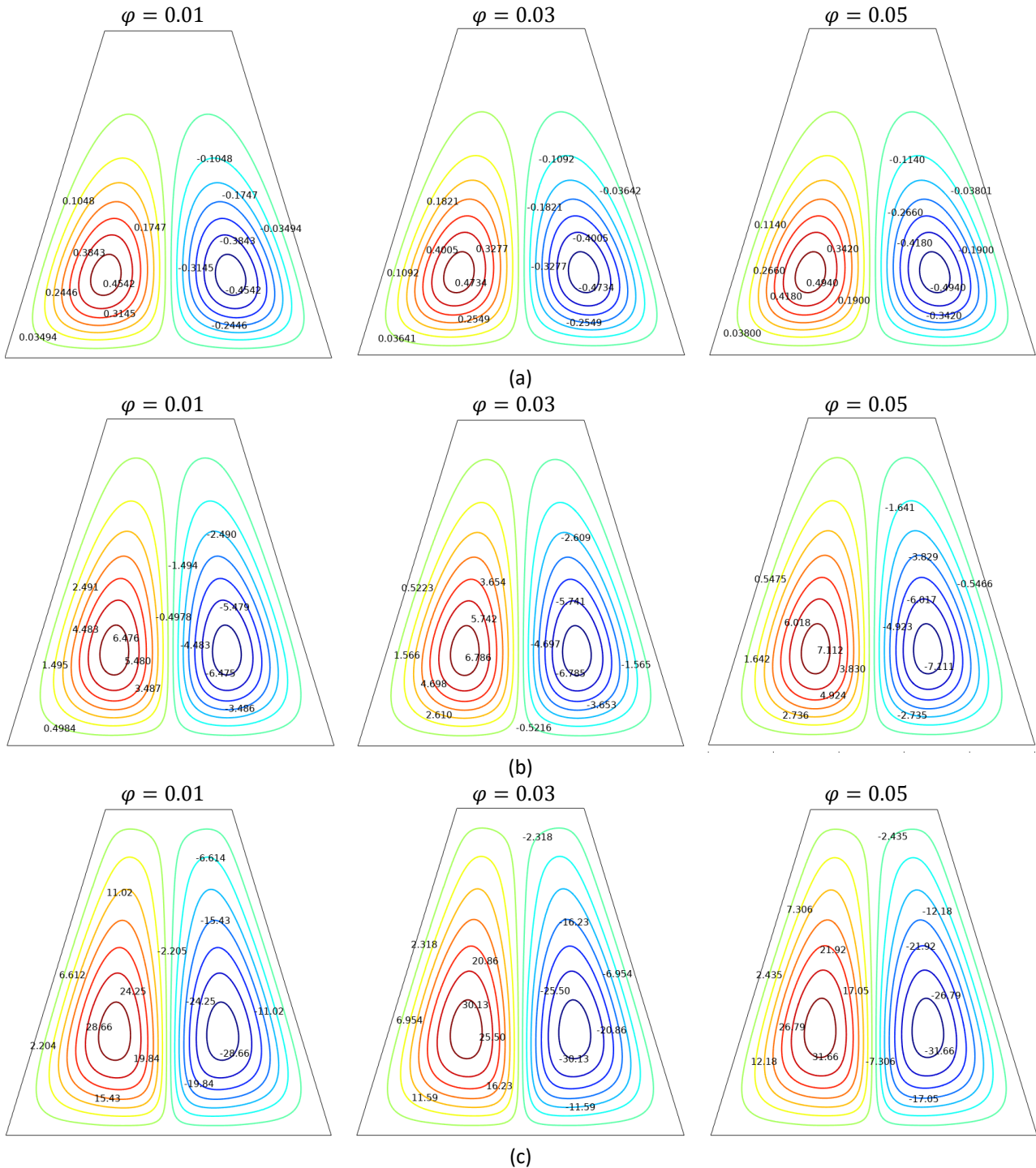
**Fig. 7.** Velocity (U) contours for different  $a$  and  $\phi$  at  $Ra = 10^5$  and  $\gamma = 1$ ; (a)  $a = 0.2$ , (b)  $a = 0.4$ , (c)  $a = 0.6$



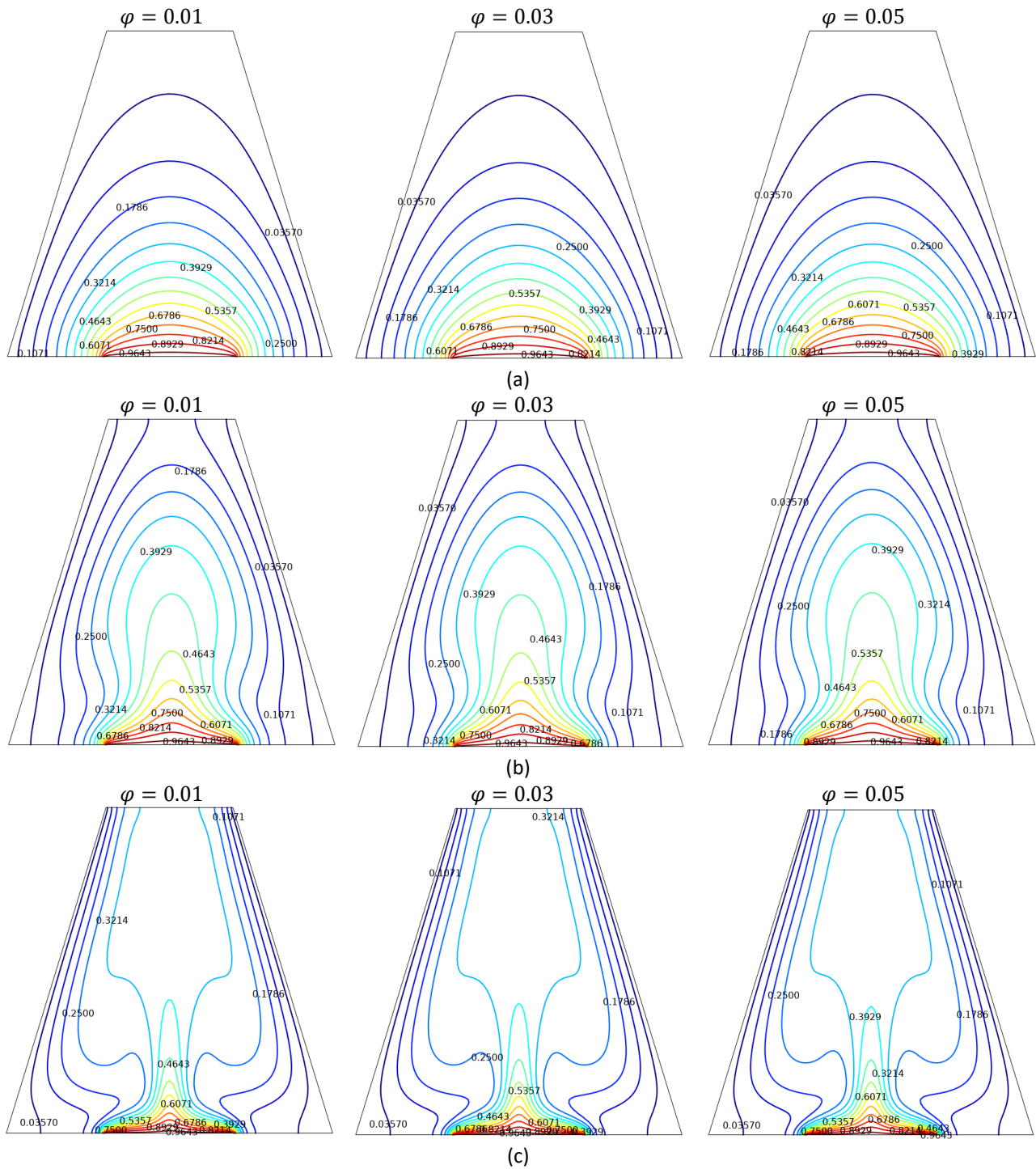
**Fig. 8.** Velocity ( $V$ ) contours for different  $a$  and  $\varphi$  at  $Ra = 10^5$  and  $\gamma = 1$ ; (a)  $a = 0.2$ , (b)  $a = 0.4$ , (c)  $a = 0.6$

Figure 9 to Figure 12 present the effects of Rayleigh number ( $Ra$ ) on streamlines, isotherms and velocities for various values of the hybrid nanoparticles volume fraction with  $a = 0.4$  and  $\gamma = 0.5$ . For  $Ra = 10^4$ , the contour maps of streamlines and isotherm show that the conduction mode dominates in the whole enclosure because of low momentum and thermal gradients. It is observed the momentum gradient increases with the increase value of  $Ra$  from  $10^4$  to  $10^6$ . Thus, the convection mode of heat transfer is increase and the fluid circulation are occupying the entire cavity. On the other hand, the size of circulation cell enlarges with high  $Ra$ . As the values of  $Ra$  increases, the convection heat transfer inside the cavity increases. In Figure 10, the thermal boundary layer

thickness near the side wall decreases with increasing values of  $Ra$ . This happen is because of the strong impact of buoyancy forces and the convection mode of heat transfer is effective in the whole cavity. Moreover, it was found that the distribution of streamlines, isotherms and velocities contour maps almost similar with various values of particles volume fraction.



**Fig. 9.** Streamlines contours for different  $Ra$  and  $\phi$  at  $a = 0.4$  and  $\gamma = 1$ ; (a)  $Ra = 10^4$ , (b)  $Ra = 10^5$ , (c)  $Ra = 10^6$



**Fig. 10.** Isotherms contours for different  $Ra$  and  $\varphi$  at  $a = 0.4$  and  $\gamma = 1$ ; (a)  $Ra = 10^4$ , (b)  $Ra = 10^5$ , (c)  $Ra = 10^6$

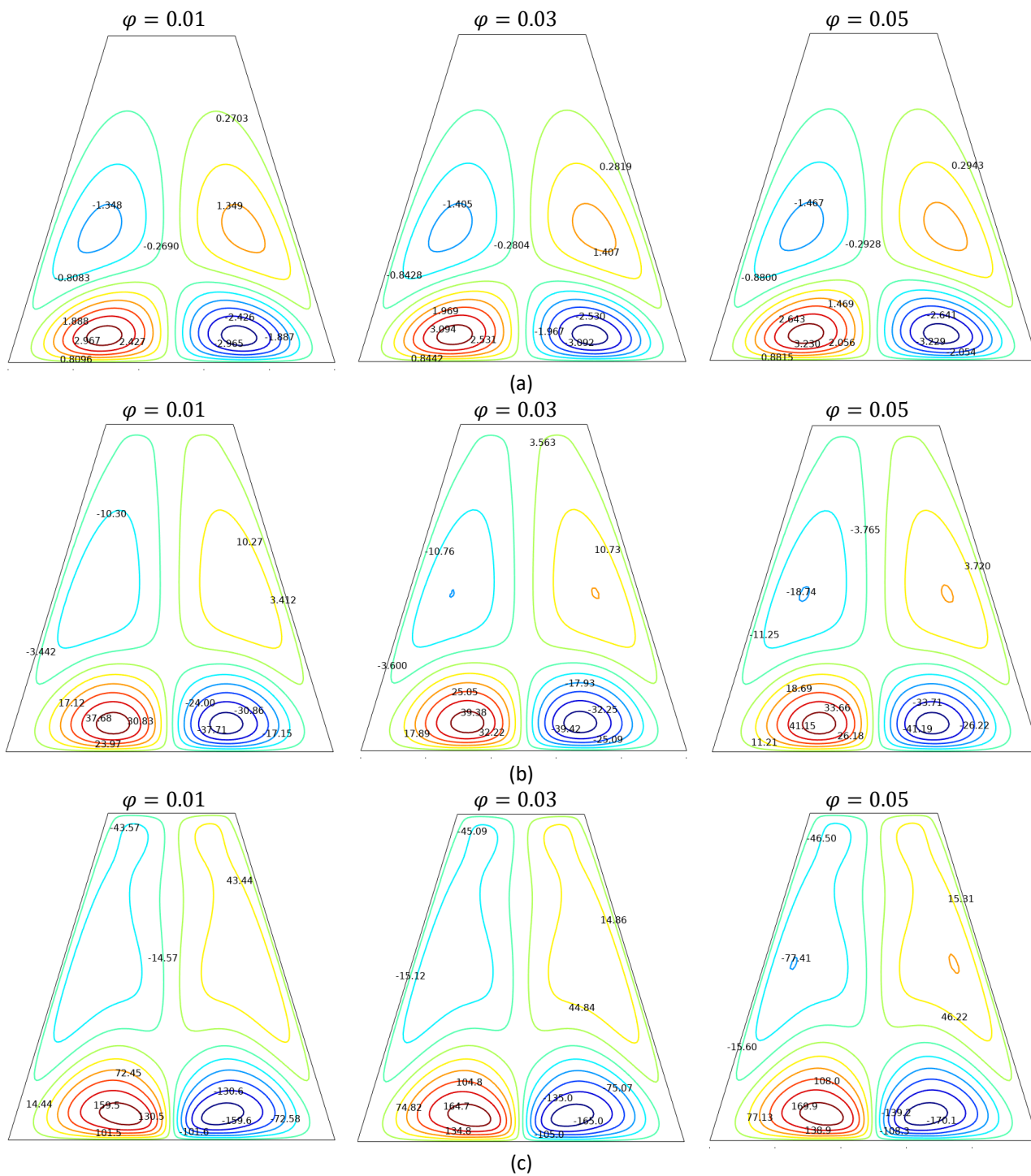


**Fig. 11.** Velocity ( $U$ ) contours for different  $Ra$  and  $\varphi$  at  $a = 0.4$  and  $\gamma = 1$ ; (a)  $Ra = 10^4$ , (b)  $Ra = 10^5$ , (c)  $Ra = 10^6$

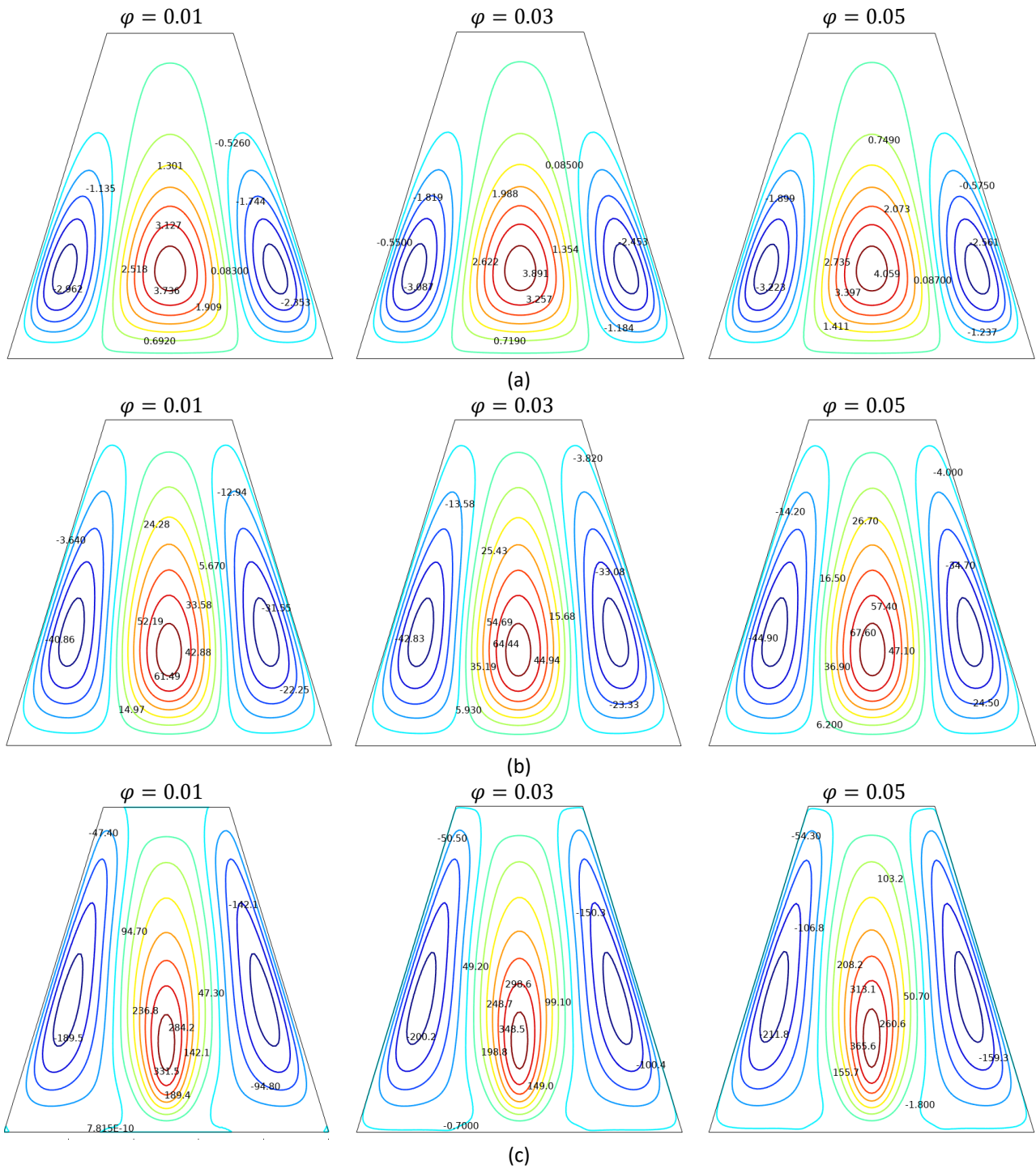


**Fig. 12.** Velocity ( $V$ ) contours for different  $Ra$  and  $\varphi$  at  $a = 0.4$  and  $\gamma = 1$ ; (a)  $Ra = 10^4$ , (b)  $Ra = 10^5$ , (c)  $Ra = 10^6$

The average Nusselt number ( $Nu_{avg}$ ) along the bottom heated surface for various values of  $\gamma$ ,  $\varphi$  and  $a$  are presented in Figure 13 to Figure 15. From these graphs, it is clearly observed that the heat transfer rate is more effective for hybrid nanofluid ( $\varphi > 0.01$ ) than the mono nanofluid ( $\varphi = 0.01$ ). When the second nanoparticles are added into the base fluid, the convection heat transfer enhances which in turn increases the thermal characteristics and the temperature distribution. For higher values of  $Ra$ , the flow circulation become stronger and  $Nu_{avg}$  is increases with the addition of nanoparticles. Hybrid nanofluids are advantageous in improving thermophysical properties and

elevating the convective heat transfer rate in comparison with mono nanofluids. Figure 13 is plotted to see the effect of Casson parameter ( $\gamma$ ) on  $Nu_{avg}$  for various value of  $\phi$ . As  $\phi$  increases lead to decrease the effective viscosity of the fluid and the overall heat transfer rate increases. Figure 14 reveal the effects of  $\phi$  and  $\gamma$  on  $Nu_{avg}$  for different values of  $a$ . It is shows that an increment  $a$  makes the  $Nu_{avg}$  increases. This happen is because of more heat is transferred to the cold wall. Thus, the strength of convection mode of heat transfer effect enhances. The variation of  $Nu_{avg}$  with different particles volume fraction is demonstrated in Figure 15. As illustrated in the figure, it is clearly observed that the thermal conductivity is enhanced with an increased the hybrid nanoparticles volume fraction and the  $Nu_{avg}$  increases. It can be concluded that the heat transfer coefficient is enhancing significantly with increase the hybrid nanoparticles volume fraction.

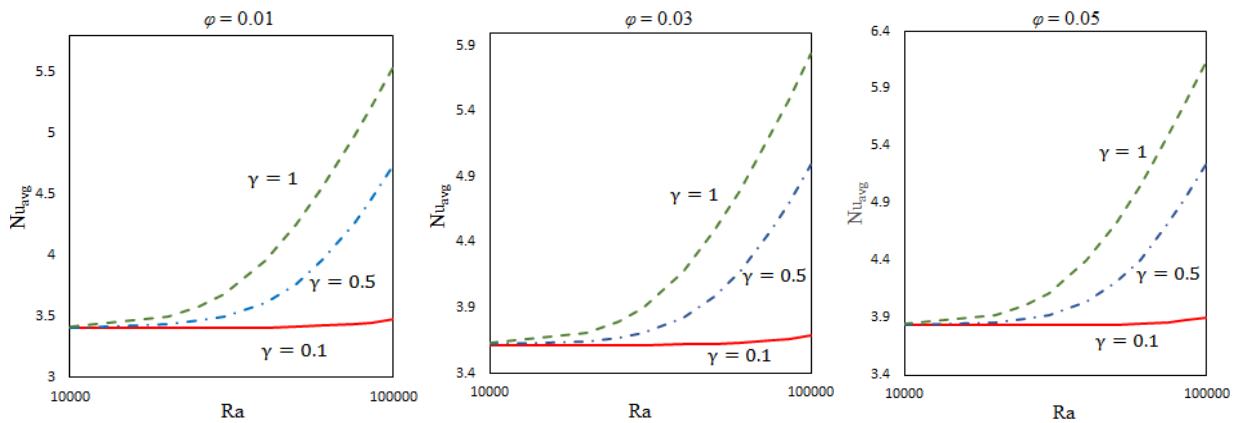


Fig. 13. Effects  $Ra$  and  $\gamma$  on  $Nu_{avg}$  with different values of  $\phi$

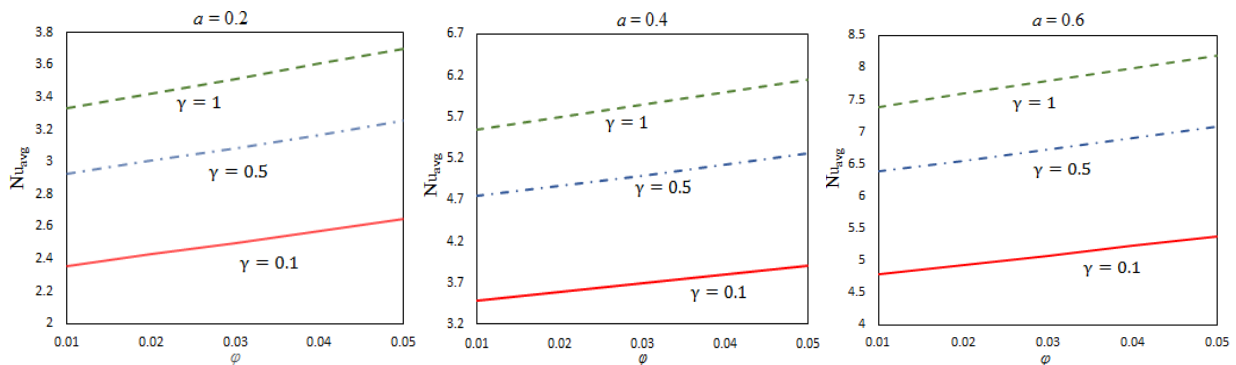


Fig. 14. Effects  $\phi$  and  $\gamma$  on  $Nu_{avg}$  with different  $a$

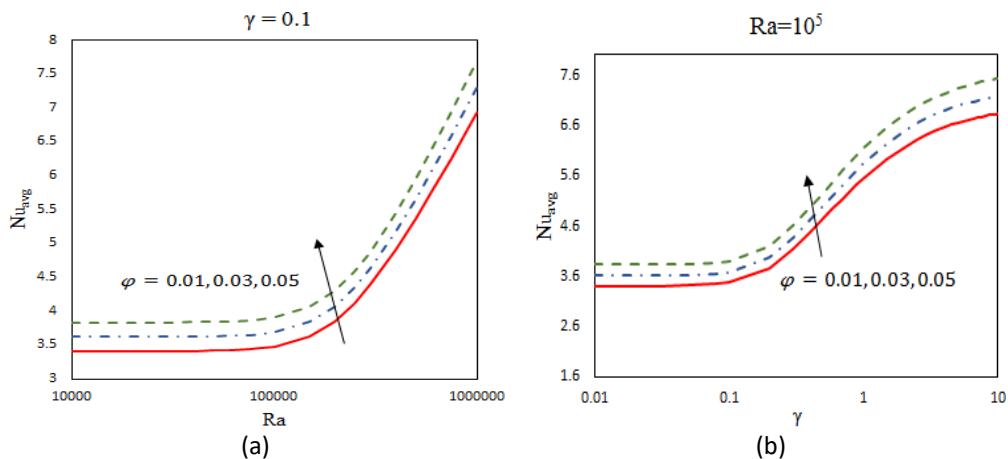


Fig. 15. Effects of (a)  $Ra$  and (b)  $\gamma$  on  $Nu_{avg}$  with different  $\phi$



## 5. Conclusions

In the present study, Casson hybrid nanofluid natural convection heat transfer in trapezoidal cavity containing a partially heated at bottom wall was numerically investigated. The results are obtained for streamlines, isotherms, velocities and average Nusselt number for different values of non-dimensional governing parameters, namely Rayleigh number ( $Ra$ ), hybrid nanoparticles volume fraction ( $\phi$ ), Casson parameter ( $\gamma$ ) and heated surface length ( $a$ ). A clear conclusion can be drawn from the numerical computational analysis

- i. The flow circulation of hybrid Casson nanofluid inside the trapezoidal cavity is stronger with the higher values of  $Ra$  and  $\phi$ .
- ii. A greater distortion of the isotherms occurs by increasing the  $Ra$  and/or increasing  $\phi$ .
- iii. The flow circulation is stronger due to large surface area of  $a$ .
- iv. The average Nusselt number are increasing with the increase of the  $Ra$  and  $\phi$ .
- v. The average Nusselt number raised as  $\gamma$  and  $\phi$  were raised.

## References

- [1] Yahaya, Rusya Iryanti, Norihan Md Arifin, and Siti Suzilliana Putri Mohamed Isa. "Stability analysis on magnetohydrodynamic flow of casson fluid over a shrinking sheet with homogeneous-heterogeneous reactions." *Entropy* 20, no. 9 (2018): 652. <https://doi.org/10.3390/e20090652>
- [2] Lund, Liaquat Ali, Zurni Omar, Ilyas Khan, and Sumera Dero. "Multiple solutions of  $\text{Cu-C}_6\text{H}_9\text{NaO}_7$  and  $\text{Ag-C}_6\text{H}_9\text{NaO}_7$  nanofluids flow over nonlinear shrinking surface." *Journal of Central South University* 26, no. 5 (2019): 1283-1293. <https://doi.org/10.1007/s11771-019-4087-6>
- [3] Salahuddin, T., Nazim Siddique, and Maryam Arshad. "Insight into the dynamics of the non-Newtonian Casson fluid on a horizontal object with variable thickness." *Mathematics and Computers in Simulation* 177 (2020): 211-231. <https://doi.org/10.1016/j.matcom.2020.04.032>
- [4] Khan, Ansab Azam, Khairy Zaimi, Suliadi Firdaus Sufahani, and Mohammad Ferdows. "MHD flow and heat transfer of double stratified micropolar fluid over a vertical permeable shrinking/stretching sheet with chemical reaction and heat source." *Journal of Advanced Research in Applied Sciences and Engineering Technology* 21, no. 1 (2020): 1-14. <https://doi.org/10.37934/araset.21.1.114>
- [5] Bilal Ashraf, M., and H. Roohani Ghehsareh. "Model of Casson fluid with Cattaneo-Chirstov heat flux and Hall effect." *Indian Journal of Physics* 95, no. 7 (2021): 1469-1477. <https://doi.org/10.1007/s12648-020-01819-y>
- [6] Mousavi, Seyed Mahdi, Mohammadreza Nademi Rostami, Mohammad Yousefi, Saeed Dinarvand, Ioan Pop, and Mikhail A. Sheremet. "Dual solutions for Casson hybrid nanofluid flow due to a stretching/shrinking sheet: A new combination of theoretical and experimental models." *Chinese Journal of Physics* 71 (2021): 574-588. <https://doi.org/10.1016/j.cjph.2021.04.004>
- [7] Yusuf, Tunde A., Rasaq A. Kareem, Samuel O. Adesanya, and Jacob A. Gbadeyan. "Entropy generation on MHD flow of a Casson fluid over a curved stretching surface with exponential space-dependent heat source and nonlinear thermal radiation." *Heat Transfer* 51, no. 2 (2022): 2079-2098. <https://doi.org/10.1002/htj.22389>
- [8] Kemparaju, M. C., Mahantesh M. Nandeppanavar, Raveendra Nagaraj, and M. Sreelatha. "Double Diffusive Casson Fluid Flow, Heat and Mass Transfer due to Porous Media with Effects of Richardson Number and Thermal Radiation." *International Journal of Applied and Computational Mathematics* 8, no. 3 (2022): 1-17. <https://doi.org/10.1007/s40819-022-01323-3>
- [9] Khan, Zeeshan, Haroon Ur Rasheed, Ilyas Khan, Hanaa Abu-Zinadah, and Maha A. Aldahlan. "Mathematical simulation of casson MHD flow through a permeable moving wedge with nonlinear chemical reaction and nonlinear thermal radiation." *Materials* 15, no. 3 (2022): 747. <https://doi.org/10.3390/ma15030747>
- [10] Varol, Yasin, Hakan F. Oztop, and Ioan Pop. "Entropy analysis due to conjugate-buoyant flow in a right-angle trapezoidal enclosure filled with a porous medium bounded by a solid vertical wall." *International Journal of Thermal Sciences* 48, no. 6 (2009): 1161-1175. <https://doi.org/10.1016/j.ijthermalsci.2008.08.002>
- [11] Sharafatmandjoor, Shervin, and C. S. Nor Azwadi. "Effect of Imposition of viscous and thermal forces on Dynamical Features of Swimming of a Microorganism in nanofluids." *Journal of Advanced Research in Micro and Nano Engineering* 7, no. 1 (2022): 8-13.

- [12] Akaje, T. W., and B. I. Olajuwon. "Impacts of Nonlinear thermal radiation on a stagnation point of an aligned MHD Casson nanofluid flow with Thompson and Troian slip boundary condition." *Journal of Advanced Research in Experimental Fluid Mechanics and Heat Transfer* 6, no. 1 (2021): 1-15.
- [13] Mahat, Rahimah, Muhammad Saqib, Imran Ulah, Sharidan Shafie, and Sharena Mohamad Isa. "MHD Mixed Convection of Viscoelastic Nanofluid Flow due to Constant Heat Flux." *Journal of Advanced Research in Numerical Heat Transfer* 9, no. 1 (2022): 19-25.
- [14] Sheremet, Mikhail A., T. Groşan, and Ioan Pop. "Steady-state free convection in right-angle porous trapezoidal cavity filled by a nanofluid: Buongiorno's mathematical model." *European Journal of Mechanics-B/Fluids* 53 (2015): 241-250. <https://doi.org/10.1016/j.euromechflu.2015.06.003>
- [15] Alsabery, A. I., A. J. Chamkha, Salam Hadi Hussain, H. Saleh, and I. Hashim. "Heatline visualization of natural convection in a trapezoidal cavity partly filled with nanofluid porous layer and partly with non-Newtonian fluid layer." *Advanced Powder Technology* 26, no. 4 (2015): 1230-1244. <https://doi.org/10.1016/j.apt.2015.06.005>
- [16] Alsabery, A. I., A. J. Chamkha, H. Saleh, and I. Hashim. "Transient natural convective heat transfer in a trapezoidal cavity filled with non-Newtonian nanofluid with sinusoidal boundary conditions on both sidewalls." *Powder Technology* 308 (2017): 214-234. <https://doi.org/10.1016/j.powtec.2016.12.025>
- [17] Pop, Ioan, and Mikhail Sheremet. "Free convection in a square cavity filled with a Casson fluid under the effects of thermal radiation and viscous dissipation." *International Journal of Numerical Methods for Heat & Fluid Flow* 27, no. 10 (2017): 2318-2332. <https://doi.org/10.1108/HFF-09-2016-0352>
- [18] Hamid, M., M. Usman, Z. H. Khan, R. U. Haq, and W. Wang. "Heat transfer and flow analysis of Casson fluid enclosed in a partially heated trapezoidal cavity." *International Communications in Heat and Mass Transfer* 108 (2019): 104284. <https://doi.org/10.1016/j.icheatmasstransfer.2019.104284>
- [19] Aneja, Madhu, Avinash Chandra, and Sapna Sharma. "Natural convection in a partially heated porous cavity to Casson fluid." *International Communications in Heat and Mass Transfer* 114 (2020): 104555. <https://doi.org/10.1016/j.icheatmasstransfer.2020.104555>
- [20] Choi, S. US, and Jeffrey A. Eastman. *Enhancing thermal conductivity of fluids with nanoparticles*. No. ANL/MSD/CP-84938; CONF-951135-29. Argonne National Lab. (ANL), Argonne, IL (United States), 1995.
- [21] Mintsu, Honorine Angue, Gilles Roy, Cong Tam Nguyen, and Dominique Doucet. "New temperature dependent thermal conductivity data for water-based nanofluids." *International Journal of Thermal Sciences* 48, no. 2 (2009): 363-371. <https://doi.org/10.1016/j.ijthermalsci.2008.03.009>
- [22] Saleh, H., R. Roslan, and I. Hashim. "Natural convection heat transfer in a nanofluid-filled trapezoidal enclosure." *International Journal of Heat and Mass Transfer* 54, no. 1-3 (2011): 194-201. <https://doi.org/10.1016/j.ijheatmasstransfer.2010.09.053>
- [23] Nasrin, Rehena, and Salma Parvin. "Investigation of buoyancy-driven flow and heat transfer in a trapezoidal cavity filled with water-Cu nanofluid." *International Communications in Heat and Mass Transfer* 39, no. 2 (2012): 270-274. <https://doi.org/10.1016/j.icheatmasstransfer.2011.11.004>
- [24] Miroshnichenko, Igor V., Mikhail A. Sheremet, Hakan F. Oztop, and Khaled Al-Salem. "MHD natural convection in a partially open trapezoidal cavity filled with a nanofluid." *International Journal of Mechanical Sciences* 119 (2016): 294-302. <https://doi.org/10.1016/j.ijmecsci.2016.11.001>
- [25] Takabi, Behrouz, and Saeed Salehi. "Augmentation of the heat transfer performance of a sinusoidal corrugated enclosure by employing hybrid nanofluid." *Advances in Mechanical Engineering* 6 (2014): 147059. <https://doi.org/10.1155/2014/147059>
- [26] Tayebi, Tahar, and Ali J. Chamkha. "Entropy generation analysis during MHD natural convection flow of hybrid nanofluid in a square cavity containing a corrugated conducting block." *International Journal of Numerical Methods for Heat & Fluid Flow* 30, no. 3 (2019): 1115-1136. <https://doi.org/10.1108/HFF-04-2019-0350>
- [27] Ghalambaz, Mohammad, Natalia C. Roşca, Alin V. Roşca, and Ioan Pop. "Mixed convection and stability analysis of stagnation-point boundary layer flow and heat transfer of hybrid nanofluids over a vertical plate." *International Journal of Numerical Methods for Heat & Fluid Flow* 30, no. 7 (2019): 3737-3754. <https://doi.org/10.1108/HFF-08-2019-0661>
- [28] Alshuraiaan, Bader, and Ioan Pop. "Numerical simulation of mixed convection in a lid-driven trapezoidal cavity with flexible bottom wall and filled with a hybrid nanofluid." *The European Physical Journal Plus* 136 (2021): 580. <https://doi.org/10.1140/epjp/s13360-021-01349-4>
- [29] Sadeghi, Mohamad Sadegh, Naghmeh Anadolibkhan, Ramin Ghasemiasl, Taher Armaghani, Abdul Sattar Dogonchi, Ali J. Chamkha, Hafiz Ali, and Amin Asadi. "On the natural convection of nanofluids in diverse shapes of enclosures: an exhaustive review." *Journal of Thermal Analysis and Calorimetry* 147 (2020): 1-22. <https://doi.org/10.1007/s10973-020-10222-y>